Tropical Forest Measurement by Interferometric Height Modeling and P-Band Radar Backscatter

Till Neeff, Luciano Vieira Dutra, João Roberto dos Santos, Corina da Costa Freitas, and Luciana Spinelli Araujo

Abstract: A new approach to tropical forest biomass monitoring with airborne interferometric X and P-band synthetic aperture radar (SAR) data is presented. Forest height, basal area, and aboveground biomass are modeled from remote sensing data for a study site in the Brazilian Amazon. Radar data quality has improved: A novel digital model of vegetation height from X- and P-band interferometry is available along with the usual P-band backscatter information. The digital vegetation height model is derived from the interferometric surface models of the ground (from P-band) and the forest canopy (from X-band). The difference between the surface models is called "interferometric height," and is used as a measure of vegetation height. Interferometric height is shown to relate to a subset of the forest trees that changes according to the forest successional stages. The suitability of radar backscatter and interferometric height as a means for forest and biomass monitoring was explored by relating forest parameters as measured in the field to remote sensing data. Basal area and biomass were related to radar backscatter with limited precision of $r^2 = 0.19$ and $r^2 = 0.34$, respectively. Mean forest height is shown to relate to interferometric height with good precision ($r^2 = 0.83$, RMSE = 4.1 m). A statistical model for forest biomass as a function of both P-band backscatter and interferometric height information not only arrives at high values of precision (with $r^2 = 0.89$ and a RMSE from cross-validation of only 46.1 t/ha), but also overcomes the well-known issue of backscatter saturation. This research shows that tropical forest biomass can be quantified and mapped over large areas for a range of forest structures with reasonably tight and similar errors. FOR. SCI. 51(6):585–594.

Key Words: Amazon, backscatter saturation, biomass, forest height, interferometric height, P-band, radar.

ADVANCED FOREST MANAGEMENT PLANNING requires knowledge of stand conditions. According to the pace of planning, inventories have to gather adequate data on the state of the forest. Biomass and timber volume are the two forest parameters of greatest importance for modern forestry. In forestry, when aiming for sustainable production of wood, utmost attention must be dedicated to timber volume. Height and basal area are the most commonly used auxiliary variables when calculating timber volume. Forest height is also needed to assess growth dynamics and site productivity. Biomass has increasingly attracted attention due to recent carbon policy development. The implications of the United Nations Framework Convention on Climate Change may entail an additional economic interest in forests and their carbon stocks. Inventory technology is highly sought after to periodically monitor forest parameters such as timber volume, forest height, basal area, and biomass.

Remote sensing is an indispensable option for forest monitoring. Traditional forest inventories that rely on fieldwork entail high costs. This is particularly true in the tropics, where forests extend over large geographic areas with difficult terrain. Intensive research efforts are dedicated to the development of remote sensing as a tool for forest measurement in the tropics. Radar is considered a powerful option for remote forest measurement in cloudy tropical environments (Hoekman and Varekamp 2001). As opposed to optical and lidar remote sensing, microwaves are not affected by atmospheric instabilities, such as light conditions and moisture content. In a study by Hyyppä et al. (2000) advanced radar products outperformed all other data types, including ground inventories and various other remote sensing tools, for forest measurement. The potential of radar as a means for tropical forest inventories has been investigated with varying success (e.g., Luckman et al. 1998; Hoekman and Varekamp 2001, Santos et al. 2002).

T. Neeff, National Institute for Space Research (INPE); University of California at Berkeley. Present address: University of Freiburg, Biometry Department, Tennenbacher Strasse 4, 79085 Freiburg Brsg., Germany—Phone: +49 (761) 203-8652; Fax: +49 (761) 203-3751; till@neeff.com. L.V. Dutra, National Institute for Space Research (INPE), Av. dos Astronautas 1758, 12.227-010 São José dos Campos (SP), Brazil—Phone: +55 (12) 3945-6444; dutra@dpi.inpe.br. J.R. dos Santos, National Institute for Space Research (INPE), Av. dos Astronautas 1758, 12.227-010 São José dos Campos (SP), Brazil—Phone: +55 (12) 3945-6427; jroberto@ltid.inpe.br. C.C. Freitas, National Institute for Space Research (INPE), Av. dos Astronautas 1758, 12.227-010 São José dos Campos (SP), Brazil—Phone: +55 (12) 3945-6475; corina@dpi.inpe.br. L.S. Araujo, National Institute for Space Research (INPE), Av. dos Astronautas 1758, 12.227-010 São José dos Campos (SP), Brazil—Phone: +55 (12) 3945-6427; lucian@ltid.inpe.br.

Acknowledgments: The authors acknowledge Conselho Nacional de Desenvolvimento Científico e Tecnológico (Grants 301400/91-1(PV), 300677/91-0, 380597/99-3, 300927/92-4), Fundação de Amparo à Pesquisa do Estado de Minas Gerais (Grant CRA 00054/00) support, and funds from the MCT (Brazilian Ministry of Science and Technology), within its program "Science & Technology for Environmental Studies." The authors thank the 8th BEC (Brazilian Army), IBAMA/MMA, and SUDAM for logistic support. This research is a partial result of the LBA LC-11 project and also of the scientific cooperation among the INPE (National Institute for Space Research), DSG (Brazilian Army Geographical Service), and UCB (University of California at Berkeley). Thanks to the anonymous reviewers whose comments helped to improve the manuscript.

Manuscript received July 3, 2003, accepted June 10, 2005

For biomass retrievals, a statistical relationship between radar backscatter and biomass from fieldwork is commonly used (Le Toan et al. 1992). Saturation of backscatter at high biomass stocks is recognized as a general problem associated with radar. With increasing biomass levels, large differences in biomass would result in decreasing differences of radar intensity. The saturation effect is particularly pronounced at higher frequencies, but even very long P-band wavelengths present a universal saturation point of 100–200 t/ha (Imhoff 1995). Therefore, investigations have focused on vegetation types with lower biomass. Even though conventional radar that only provides the backscatter information is capable of monitoring forest regeneration and growth, the usefulness of large-scale biomass inventories is considerably limited (Imhoff 1995). This is why Dobson et al. (1995) estimate basal area and height separately and combine them in a biophysically meaningful model for biomass prediction. Conventional radar approaches suffer from a lack of information on a conceptually convincing predictor of forest biomass (Treuhaft and Siqueira 2004).

More advanced radar techniques have been suggested to overcome the limitations of raw synthetic aperture radar (SAR) intensity for forest measurement. Treuhaft and Siqueira (2004) advocate the use of interferometric SAR for forest structure and biomass estimation. Interferometric SAR data sets can include components with different observational characteristics (Treuhaft and Siqueira 2004), i.e., with multiple baselines (Treuhaft and Siqueira 2000), multiple polarizations (Papathanassiou and Cloude 2001), or multiple frequencies (this article). In comparing a suite of different radar methods for forest measurement, Hyyppä et al. (2000) recommend the use of the coherence techniques, which yield superior data in comparison to standard radar approaches. Koskinen et al. (2001) suggest the integration of both intensity and coherence data, because these contain complementary information regarding the physical and phenomenological conditions of ground and vegetation cover. Treuhaft and Siqueira (2004) depict the advantage of estimating forest structural features from the interferometric coherence and phase observations to express biomass as a function of these, rather than as a function of the backscatter only. Estimation of biomass reflects the estimation of height and basal area (Hyyppä et al. 2000).

In this context, the estimation of forest height from interferometric radar and links to biomass has received increasing attention (Hoekman and Varekamp 2001, Treuhaft and Siqueira 2000, Papathanassiou and Cloude 2001). SAR-based forest height measurements are a conceptually promising predictor of forest structure and biomass. Papathanassiou and Cloude (2001) used polarimetric SAR interferometry along with a scattering model to derive vegetation height from the differences in the scattering mechanisms between vegetation layers and the ground. Treuhaft and Siqueira (2000) compared two-baseline interferometry and polarimetric interferometry for the determination of vegetation height. Hyyppä et al. (2000) explored the performance of radar-derived stand profiles, and concluded that height from the radar profiles was the best single predictor of forest structure and biomass.

In this article, the performance of single-baseline multifrequency interferometric SAR for forest measurement is examined. The approach incorporates vegetation height information and microwave rather than optical or laser technology. Both interferometric vegetation height and P-band backscatter, as derived from interferometric SAR, are combined in a biomass model. Interferometric height is derived from the difference of X- and P-band digital surface models, and its additional incorporation is aimed to overcome the restriction of mere backscatter information to forest types with low biomass volumes. Addressing forest biomass using such conventional radar systems creates similar shortcomings to measuring biomass only by basal area: Precision is fairly limited. In ground inventories, biomass is usually computed as a function of both basal area and tree height. Hence, in remote sensing inventories both backscatter and interferometric height can be used to establish a "natural" approach to biomass modeling.

Materials and Methods

Study Area

The study area is situated in the Tapajós National Park south of Santarém in the Brazilian Amazon, at W54.9°, S3.1°. The climate according to Köppen is *Amw* (variation of tropical monsoon) with an average annual rainfall of 1,750–2,000 mm and a yearly temperature average of 26°C.

The natural vegetation consists of tropical lowland forest, mainly dense forest with emergents. Characteristic species include *Carapa guianensis* Aubl., *Eschweilera odora* (Poepp) Miers., *Couratari* sp., *Tachigalia myrmecophylla* Ducke, *Coumarouma odorata* Aubl., and *Nectandra mollis* Nees. The area encompasses forests in a number of successional stages ranging from primary forest, over advanced and intermediate regrowth, to recently cut fallows. Forest degradation mainly results from felling for agriculture, selective logging, and fire. Major species of secondary vegetation include *Cecropia* sp., *Vismia guianensis* (Aubl.) Choisy, *Guatteria poeppigiana* Mart., and *Didymopanax morototoni* Aubl.

Ground Data

Extensive fieldwork was conducted to collect data on primary and second-growth forests in 1995, 1999, and 2000. In 1995 three plots of second-growth forest were measured with plot areas of 200 m^2 each. A total of 44 plots were measured in 1999 and 2000; 16 of which corresponded to primary forest with plot areas of 2,500 m^2 each. The rest corresponded to various stages of second-growth forests, with plot areas of 1,000 m^2 each. Field measurements included tree positions, species, diameter at breast height, and total tree heights for all trees with diameters greater than 5 cm in second-growth and 10 cm in primary forest. Because the availability of all types of remote sensing data is limited to a subregion of the study area, only 19 plots of

ground data could be used for the final model; 9 of these corresponded to primary forest and 10 to second-growth forest. Backscatter data are available for 37 plots, and for 23 plots interferometric height data are available.

The data allow for the computation of standard forest parameters for diameter, basal area, and height as defined by Loetsch et al. (1973) for both the whole set, and separately for second-growth and primary forest. Various height measures were computed (mean, median, predominant height, and "subemergent height") and biomass was derived by different allometric equations.

The concept of predominant height h_{dom} builds on taking the arithmetic mean of only a subset of the tallest individuals, such that $h_{\text{dom}} > \bar{h}$ (Loetsch et al. 1973). Predominant height, i.e., the mean height of the tallest trees in a stand, was computed for the tallest 20%, and the tallest 100 and 200 individuals per hectare. In addition to predominant height, subemergent height h_{sub} is defined here to be the arithmetic mean of only a subset of the smallest individuals: $h_{\text{sub}} < \bar{h}$; subemergent height is not a common height measure for forests. So, h_{dom} and h_{sub} are a summation over j individuals for stand i:

$$h_{\text{dom}} = \frac{1}{n_i} \sum_{h_{ij} < h_{\min_i}}^{n_i} h_{ij}, \quad h_{\text{sub}} = \frac{1}{n_i} \sum_{h_{ij} < h_{\max_i}}^{n_i} h_{ij}, \qquad (1)$$

where $h_{\min_i}$ or $h_{\max_i}$, and thus n_i needs be determined for each stand, by either including a certain percentage or including a certain number of trees per hectare from the upper (dom) or lower (sub) end. The concept of predominant and subemergent height measures is illustrated in Figure 1. In the case of primary forest, those trees that are part of a tallest collective are representative for the stand. They prevail in the sense that their crowns constitute the canopy, and smaller trees create the understory. It is also recognized that, in second-growth forest, this representative collective consists in the smallest trees of a stand; taller individuals are emergents.

Biomass was estimated using allometric equations drawing on the diameter $d_{1.3}$, namely one for second growth described by Nelson et al. (1999) and a different one for primary forest published by Chambers et al. (2001). All data in this article refer to *standing alive aboveground biomass* only. Other biomass fractions are not accounted for.

$$\log(\text{biomass}) = -0.370 + 0.333 \cdot [\log(d_{1.3})] + 0.933 \cdot [\log(d_{1.3})]^2 - 0.122 \cdot [\log(d_{1.3})]^3, \qquad (2)$$

(Chambers et al. 2001)

$$\log(\text{biomass}) = -1.9968 + 2.4128 \cdot [\log(d_{1.3})]. \qquad (3)$$

(Nelson et al. 1999)

The biomass and height data from 1995 were corrected to retrieve presumable forest conditions in 2000, when the remote sensing data were acquired. Corrected values come from a growth model for secondary forest in the Tapajós region (Neeff and dos Santos, 2005) that has been derived from a set of data similar to those used here. The stand to be corrected is attributed a physiological age by its top height, increments in biomass or height for the subsequent time period can be derived from the model.

Remote Sensing Data

An area of approximately 1,300 km^2 was mapped at the end of 2000. The data were collected by the airborne AeS-1 sensor (Aerosensing Radarsysteme GmbH, Oberpfaffenhofen, Germany), which makes use of interferometric synthetic aperture radar (InSAR) technology. It operates on

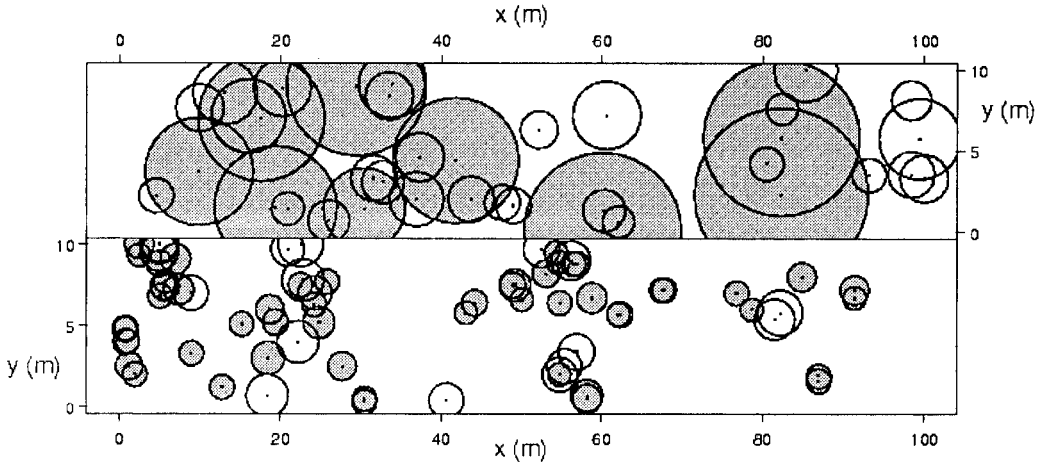

Figure 1. The concept of predominant and subemergent forest height measures. Displayed are two transects (part of #6, and #14) resulting from fieldwork. The coordinate system refers to local transect coordinates, diameters of circles correspond to diameters of individual trees. Upper plot: primary forest, trees among the 25% tallest trees are in gray. These trees would be included in the computation of a predominant height measure. Lower plot: secondary forest, trees among the 75% smallest trees are in gray. These individuals would be part of a subemergent height measure.

X-band (9.55 GHz) with one polarization (HH) and fully polarimetric on P-band. The technical properties of the P-band were wavelength 72 cm, middle frequency 415 MHz, depression angle 45° (37–51°), mean flight height 3,216 m, range resolution 1.5 m, azimuth resolution 0.7 m for 1 look slant range image (Hofmann et al. 1999). The images were radiometrically calibrated using eight corner reflectors and the backscatter coefficients were derived (see Dutra et al. (2002) for details on processing and calibration of the data).

The longer wavelengths pass through the vegetation cover and are used to generate a digital elevation model (DEM). The short wavelengths are reflected from the top of forest canopies and are used to generate a digital surface model (DSM). Both models have a spatial resolution (pixel size) of 2.5 m. The calibration procedure (Dutra et al. 2002) draws on the differences between DEM and DSM. A local bias remains that, among other reasons, might be due to shifts of the elevation of the scattering center according to the density of vegetation. The difference between the DSM and the DEM is taken to represent height of vegetation. This height measure of vegetation is called *interferometric height.*

Results

Interferometric Height and Ground Height

In Figure 2, a scatterplot of mean forest height $\bar{h}$, as derived from ground data, versus interferometric height h_{int}, as derived from remote sensing data, is drawn. A simple linear regression yields a high coefficient of determination at $r^2 = 0.83$ and coefficients that are significantly different from the diagonal line ($\hat{\beta}_0 = 5.9$, with standard error 0.7, and $\hat{\beta}_1 = 0.5$, with standard error 0.05). The RMSE between mean forest height from fieldwork and interferometric height amounts to 4.1 m, but the RMSE between predictions of the linear regression model and field observations is only 1.8 m. Interferometric height is lower than mean forest height in initial second growth, and exceeds mean forest height at more advanced successional stages. Even though the existence of a statistical relationship between interferometric height and forest height is clear, interferometric height reflects different forest features at the successional stages.

Various standard height measures for forest stands (mean height, predominant height of the tallest 20%, and predominant height of the tallest 100 and 200 individuals per hectare) are listed in Table 1 for the field transects. A boxplot in Figure 3 shows the distributional characteristics of the same data. When comparing remote sensing data and field data, interferometric vegetation height as derived from the difference of DSM and DEM proved to be quite similar to the mean height for second growth. Furthermore, it resembles predominant height of the tallest 200 individuals per hectare for primary forest. Primary and second-growth forests appear very differently within the plot. The stratification by primary and second-growth forests not only decreases variability, but also allows the interferometric height to attain the same numerical values as the height from field measurement. Figure 3 suggests a relationship between interferometric height and different height measures for primary and secondary forests.

Figure 4 displays the dependence of interferometric height on the forest conditions. Interferometric height for primary forest is a measure of the height of a certain predominant collective h_{dom}. Interferometric height for second growth is a measure of the height of a certain subemergent collective h_{sub}. The proportions of the collectives vary

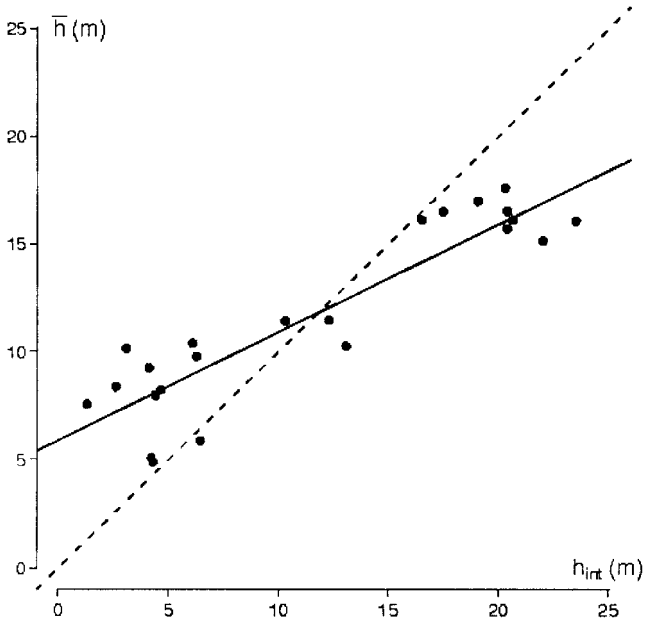

Figure 2. Scatterplot of mean forest height $\bar{h}$ from field measurement versus interferometric height h_{int} from remote sensing with linear regression line. The dashed diagonal line is included for reference.

Table 1. Various standard height measures for forest as obtained from field data, grouped by secondary (sec) and primary (pri) forest

No.	Type	$\bar{h}$	$h_{20\%}$	h_{100}	h_{200}
		(m)			
1	pri	16.1	24.3	24.5	21.4
2	pri	17.0	24.9	24.6	21.6
3	pri	16.1	24.7	24.5	21.4
4	pri	15.2	24.3	23.8	20.1
5	pri	16.5	26.3	25.6	21.7
6	pri	17.6	28.1	26.4	22.4
7	pri	16.1	25.8	23.8	20.2
8	pri	11.5	16.1	16.1	16.1
9	pri	10.3	14.0	14.0	14.0
10	sec	9.3	17.0	17.0	13.9
11	sec	8.0	11.7	13.0	12.2
12	sec	9.8	18.5	22.5	18.8
13	sec	5.9	7.1	7.1	6.7
14	sec	4.9	7.1	7.5	6.8
15	sec	8.4	11.7	12.9	12.1
16	sec	5.1	8.3	6.1	5.1
17	sec	8.2	12.0	14.1	12.3
18	sec	10.1	15.8	17.3	15.9
19	sec	11.4	16.0	16.0	16.0

Mean height for all individuals, the tallest 20%, and the tallest 100 and 200 individuals per hectare ($\bar{h}$, $h_{20\%}$, h_{100}, and h_{200}, respectively).

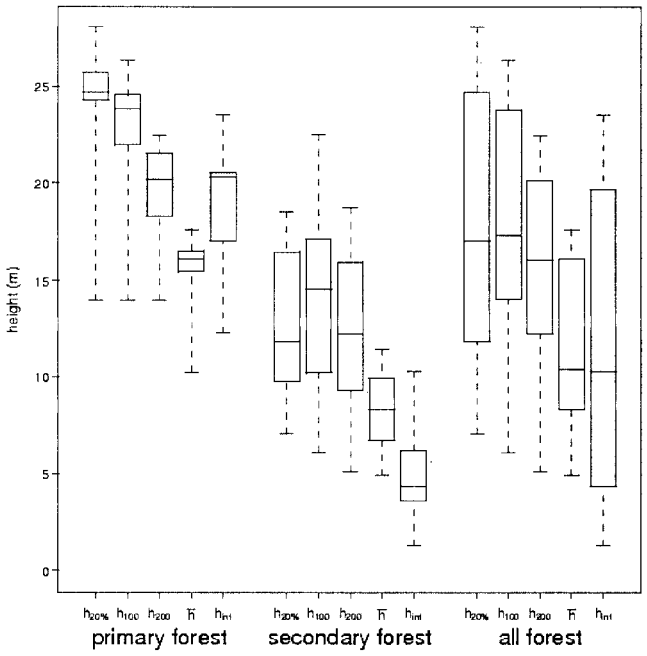

Figure 3. Boxplot of various standwise height measures as obtained from ground data and from radar data for different forest types. Displayed are predominant height (mean height of the tallest trees) of the tallest 20%, and the tallest 100 and 200 individuals per hectare, mean height, and interferometric height ($h_{20\%}$, h_{100}, h_{200}, $\bar{h}$, h_{int}, respectively) for primary forest, secondary forest, and for all forests. The box with the bar stands for ¼, ½, and ¾ quantiles, and whiskers extend to the most extreme data points.

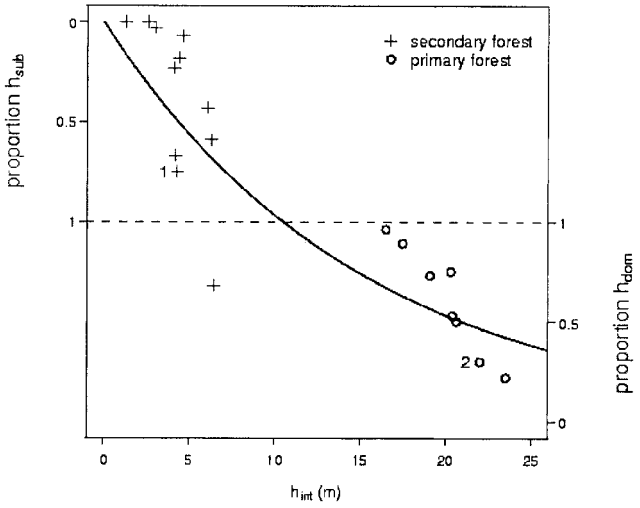

Figure 4. Proportions of predominant height h_{dom} and subemergent height h_{sub} for primary and secondary forest that equal interferometric height h_{int}. The dashed horizontal line corresponds to the arithmetic mean of all individuals. Values below the line correspond to the proportion of the tallest individuals whose mean equals the interferometric height. Values above the line correspond to the proportion of the smallest individuals whose mean equals the interferometric height. The solid trend line results from exponential least-squares. Example points marked with numbers in the plot: (1) second-growth forest (sample #12) with h_{int} = 6.5 m, proportion is 0.68, i.e., the arithmetic mean of the 68% smallest trees (h_{sub}) equals h_{int}; (2) primary forest (sample #3) with h_{int} = 22.0 m, proportion is 0.30, i.e., the arithmetic mean of the 30% largest trees (h_{dom}) equals h_{int}. When the solid trend line crosses the dashed horizontal line, interferometric height equals the standard arithmetic mean height.

according to the forest conditions. Here, the dependence on interferometric height itself is displayed. In secondary forests, the interferometric height is low, and corresponds to the mean height of a subemergent collective of all trees, excluding the taller ones. With advancing succession, interferometric height increases and the subcollective grows. At a height of ~10 m, it is composed of all trees of the forest. In primary forests, the interferometric height is ~20 m, and again reflects only a subcollective of all trees, corresponding this time, however, to the predominant individuals. Unfortunately, the data set contains only a few medium-height forests. Thus, the transition between predominant and subemergent height cannot be reliably established until further data are analyzed. Nevertheless, the transition appears seamless and the data available allow for the fitting of a continuous function.

An exponential curve is fitted to assess the quality of the relationship. There is no physical necessity for preferring this functional form over others, but the exponential has some characteristics that are desired here. A sensible functional form would cross the (0, 0) point in the upper left corner, and asymptotically approach the x axis. The curve must pass the (0, 0) point because, when h_{int} is equal to zero (ground height), there are no trees being measured, i.e., the proportion of the trees in h_{sub} is equal to zero as well. The curve must not cross the lower x axis because the proportion of the trees in h_{dom} would fall below zero. The regression line displayed in Figure 4 results from fixing the intercept (thus the coefficient of determination is meaningless and not given here).

Figure 2 shows that interferometric height and forest height are closely related. However, interferometric height overestimates mean forest height at more advanced successional stages and in primary forest, whereas it tends to underestimate initial succession. Figure 3 suggests that the use of the same forest height measure for any successional stage would confound the analysis. Nevertheless, Figure 4 illustrates that interferometric height relates to a subcollective of all trees in the forest, whose composition changes seamlessly as a function of forest condition. Figure 1 supports this observation by visual comparison of a primary forest and a second-growth stand. When excluding the understory from primary forest or emergent tree individuals from secondary forest, prevailing subcollectives are formed. Whether this subcollective is a predominant or a subemergent one depends on the forest's successional stage.

Biomass, Basal Area, and P-Band Backscatter

P-band backscatter data are related statistically to biomass and basal area of the ground data. Logarithmic functions have proved to be suitable for relating backscatter to biomass stocks, especially in cross-polarized long wavelength data (Le Toan et al. 1992). In Figure 5 scatterplots are drawn together with the respective regression lines. The coefficient of determination attains a value of $r^2 = 0.19$ for basal area and of $r^2 = 0.34$ for biomass.

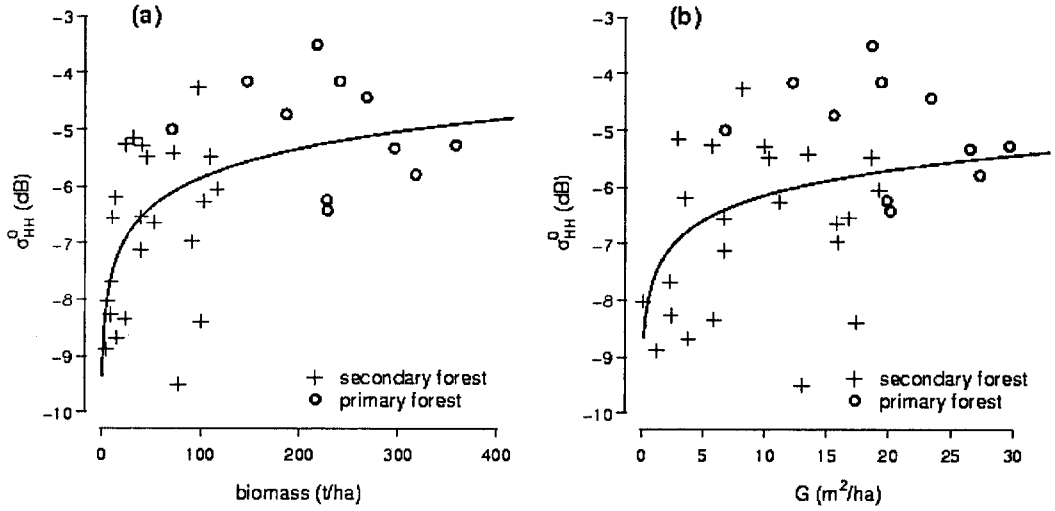

Figure 5. The backscatter saturation effect for forest biomass and total basal area. (a) Scatterplot of radar backscatter σ_{0HH} versus forest biomass. (b) Scatterplot of radar backscatter σ_{0HH} versus total basal area *G*. Points are distinguished by primary and second-growth forest, and logarithmic regression curves are displayed.

The backscatter saturation effect can be observed in the plots (Figure 5). Logarithmic functions are characterized by a decreasing slope with increasing values of the independent variable. Hence, for higher biomass levels, the use of such a relation to distinguish biomass classes is quite limited. Backscatter saturation here occurs at ~100 t/ha (and at backscatter levels of $\sigma_{0HH} \approx -6$ dB), which coincides with values obtained by other researchers (e.g., Imhoff 1995) for P-band radar data. The response of backscatter to total basal area saturates around 15 m^2/ha, which is about the same backscatter level ($\sigma_{0HH} \approx -6$ dB) as for biomass. The plots for backscatter versus biomass and basal area (Figure 5a, b) are very similar, as are the regression lines. Because biomass for forest inventories is commonly derived by allometric equations that are largely a function of basal area, it might make more sense here to depict a saturation of backscatter response to basal area rather than to biomass itself. What actually saturates the backscatter response is an increased level of total basal area.

Interferometric Height, P-Band Backscatter, and Biomass

Biomass stocks from field data are predicted by remote sensing data. First, individual relations to radar backscatter and interferometric height are examined, then both are combined in a final biomass model. Biomass stocks as obtained by various allometric equations were logarithmically related to P-band backscatter data in HH polarization (see Figure 6a). Using the allometric equation by Nelson et al. (1999) for second-growth and the equation by Chambers et al. (2001) for primary forest, a coefficient of determination of $r^2 = 0.34$ was obtained. Interferometric height, i.e., the difference between DSM and DEM, was taken to represent

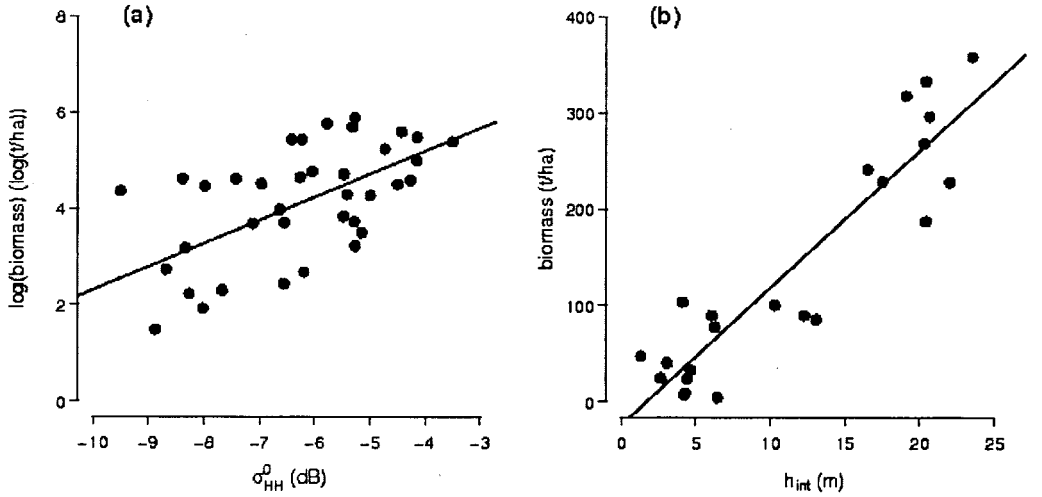

Figure 6. Relationship of biomass to remote sensing data for measured forest stands. Displayed are scatterplots with regression lines: (a) biomass on logarithmic scale versus radar backscatter σ_{0HH}; (b) biomass versus interferometric height h_{int}.

vegetation height and was related to biomass as arrived at by the same allometric equations as for the backscatter data (see Figure 6b). Height is expected to be related linearly to volume of trees (Loetsch et al. 1973), even though the scatterplot is not very clear regarding linearity. When fitting a linear function, the coefficient of determination amounts to $r^2 = 0.84$. Both backscatter and interferometric height are related to forest biomass in distinct ways.

Finally, both P-band HH backscatter σ_{0HH} and interferometric height h_{int} were fitted to biomass levels. The precision increased to $r^2 = 0.89$. The regression equation is a combination of the two individual functions. The intercept is not significantly different from 0 at the level $\alpha = 0.1$. However, there is no reason to drop the intercept from the model. This biomass model was established for all types of forest occurring in the study region, ranging from initial regrowth with biomass levels below 5 t/ha to primary forest with biomass levels up to ca. 350 t/ha:

$$\begin{array}{lccc} \text{biomass} = 44.965 + 13.87 \cdot h_{int} + 10.566 \cdot \sigma_{0HH}, & & & \\ \text{(std. error)} \quad (5.83) & (1.6) & (7.2) & \end{array} \tag{4}$$

with units: biomass − t/ha, h_{int} − m, and σ_{0HH} − dB.

In Figure 7 the final biomass model is graphically displayed as a three-dimensional surface plot. Saturation of the predictor variable cannot be observed. This model incorporates additional information from interferometry that became available due to recent advances in radar technology, namely the interferometric vegetation height, which in turn remains unaffected by the well-known radar backscatter saturation effect.

Validation of the Biomass Model

Because only few full data points are available, leave-one-out cross-validation was conducted to check how well the final model generalizes to new data and to prove the general validity of the biomass model. With the data set consisting of n runs, leave-one-out cross-validation fits the model equation to $n - 1$ runs, and predicts from the model for the omitted data point. These predictions are compared to the recorded data values to retrieve n prediction residuals. The cross-validation error of prediction corresponds to the root-mean-squared prediction residuals, and it is closely related to the PRESS (predicted residual sum of squares) statistic.

Generalization errors turned out to be small. In Figure 8a, the prediction residuals are plotted. The error of prediction is calculated as 46.1 t/ha (data range ~5–350 t/ha). A scatterplot of predicted versus observed biomass levels is displayed in Figure 8b. The corresponding linear model yields coefficients that are not significantly different from the diagonal line ($\hat{\beta}_0 = 4.3$, and $\hat{\beta}_1 = 0.97$, with standard errors 17.5 and 0.1, respectively). The results of the cross-validation procedure provide confidence in the general validity of the established biomass model.

Discussion

The analysis proposes a new approach to the monitoring of forest structure and biomass in the tropics based on the use of dual-frequency interferometric SAR. Both P-band radar backscatter and interferometric height are combined in an empirical biomass model. It entails the advantages of radar over optical data in respect of its stability toward varying atmospheric conditions. Also, the approach is much simpler and easier to conduct than photogrammetric modeling techniques. Saturation of the radar response to increasing biomass levels as in conventional radar technology that solely base on the backscatter was not observed, but the

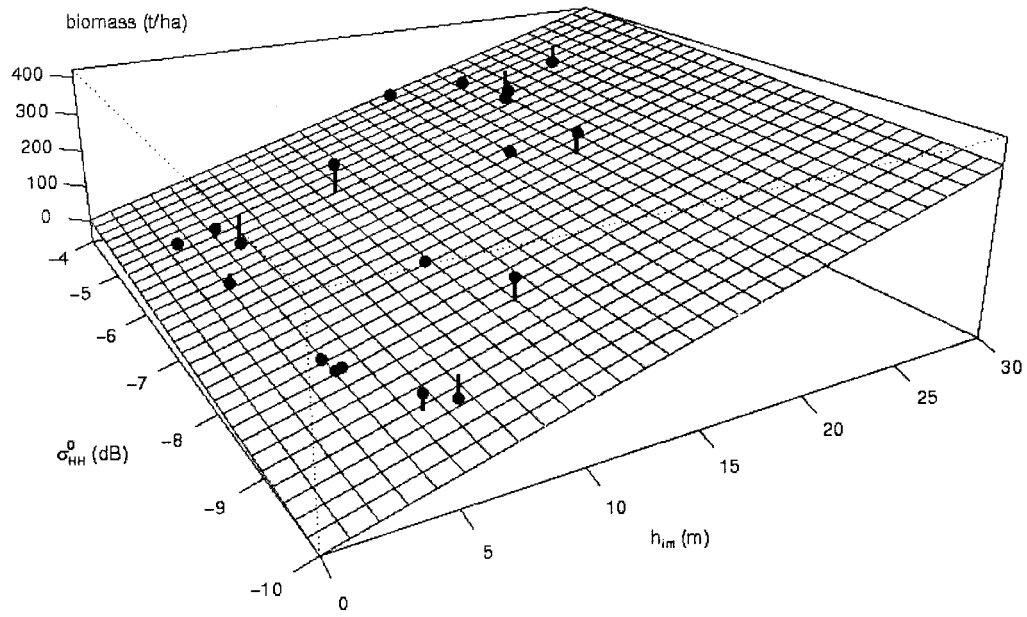

Figure 7. The final biomass model with biomass as a function of radar backscatter σ_{0HH} and interferometric height h_{int}. A grid of fitted values from the regression is displayed as a three-dimensional surface plot. Data points (bullets) are added along with residuals (bars at bottom/top of the bullets).

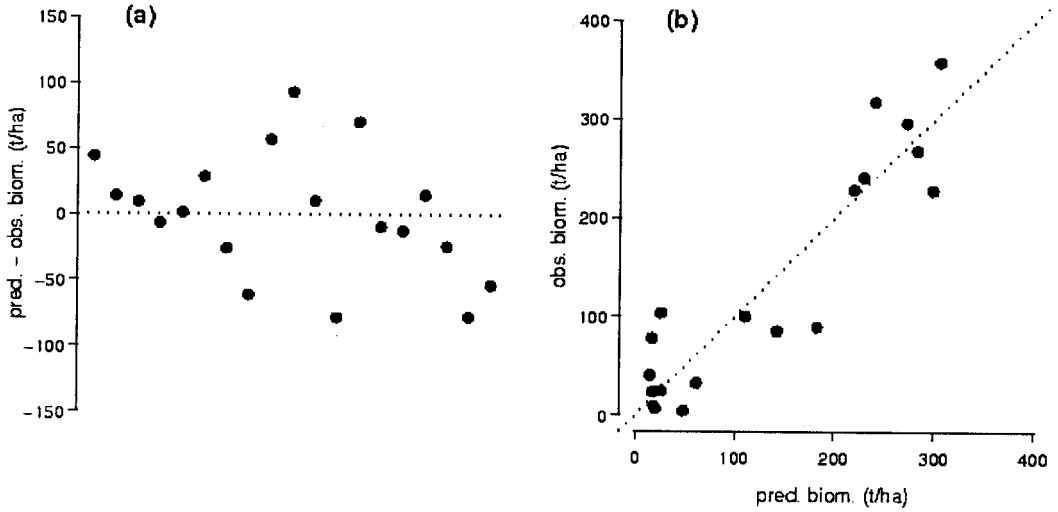

Figure 8. Cross-validation of the final biomass model. (a) Cross-validation residuals of the model. (b) Scatterplot of observed versus predicted biomass levels, with diagonal line.

established model determines biomass in forests up to ~350 t/ha. The improvement over other approaches to radar-based forest monitoring is mainly due to the incorporation of interferometric height measurements.

Interferometric vegetation height is the difference between a DSM of the forest canopy from X-band interferometry and a DEM of the ground from P-band interferometry. The system for forest height measurement builds on multiple frequency interferometric SAR, and when compared to field data, the RMSE amounts to 4.1 m. In boreal and temperate forests, other radar-based technologies for forest height measurement were tested with comparable accuracies. Hyyppä et al. (2000) report a RMSE of 3 m using radar profiles, Papathanassiou and Cloude (2001) achieve a RMSE of 2.5 m with polarimetric interferometry, and Treuhaft and Siqueira (2000) develop an approach of multibaseline polarimetric interferometry to arrive at an error of 4.2 m. The presented performance of the dual-frequency interferometric SAR for forest height estimation is notable regarding the wide ranges of different forest types it relates to and the complexity of tropical forest canopy structure that considerably complicates interferometric measurements (Hoekman and Varekamp 2001).

Interferometric height has been shown to relate to a continuously varying subset of the whole collective as a function of its height, i.e., of its successional stage. In Figure 9 the tree heights are drawn along example transects in primary and secondary forests that were measured in fieldwork. When comparing to the interferometric height, the subcollectives that form a predominant height of the upper story in primary forest (Figure 9a) and a subemergent height of the understory in secondary forest (Figure 9b) can be recognized. Typically, young second-growth forest is not quite uniform, but instead has many emergent trees, which are either remnants from before the clearcut or which are simply individuals of largely advanced growth (Hoekman and Varekamp 2001). These would not constitute a closed crown surface though, to reflect radar waves. Additionally,

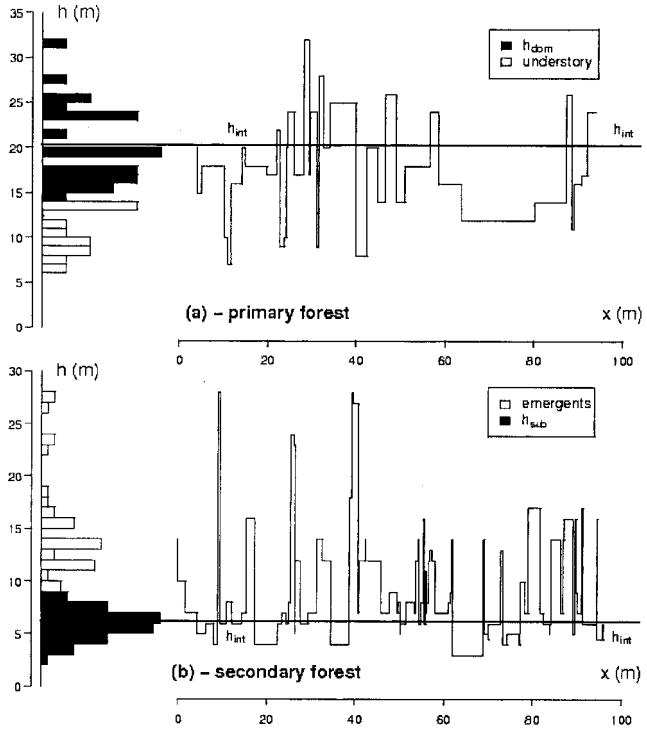

Figure 9. Relationship of interferometric height and tree heights in (a) primary forest (plot #5) and (b) secondary forest (plot #12). Displayed are heights h of trees ($d_{1.3} \geq 10$ cm in primary forest, and $d_{1.3} \geq 5$ cm in secondary forest) measured in the field along a transect line x of 100 m. The vertical line corresponds to the measured interferometric height h_{int}. The frequency distribution of the tree heights is also given. Those bars drawn in black correspond to the fraction of all trees used for computation of predominant height h_{dom} and subemergent height h_{sub}.

the height of very large emergent trees is underestimated by the interferometric technique (Hoekman and Varekamp 2001). Hence, in second-growth forest, taller individuals do not belong to the subemergent tree collective that interferometric height relates to (see Figure 9b). As forests grow older and accumulate more biomass, competition typically

results in decreasing density of individuals (this has also been observed here). Fewer individuals with more extended crowns would form a predominant collective in the upper story. Thus, X-band radar waves are reflected from the top of the crowns of the few largest individuals. Therefore, the proportion of the largest trees whose mean height corresponds to the interferometric height has been observed to drop in primary forest, and interferometric height only relates to the upper story (see Figure 9b).

The saturation of the radar intensity response with increasing biomass levels occurred at levels similar to those observed before by other researchers for P-band radar (e.g., Imhoff 1995). The behavior of biomass when related to backscatter was compared to basal area in its relationship to backscatter. The scatterplot, the statistical models, and the saturation levels of radar intensity resemble each other. This is not surprising, given that the most common allometric equations derive biomass only from basal area (Nelson et al. 1999, Chambers et al. 2001). Treuhaft and Siqueira (2004), for example, examine saturation of the radar return as a function of the density of the vegetation scatterer. Vegetation density is, in turn, associated with basal area. Indeed, Dobson et al. (1995) found good relations of radar backscatter to basal area of temperate forest stands, stipulating a high correlation between biomass stocks as derived by usual allometric equations and basal area. For long-wavelength radar data, the backscatter response relates primarily to the forest's basal area rather than to biomass itself.

The adopted biomass modeling approach is conceptually convincing because it incorporates both the radar intensity and the interferometric height, which can be associated with forest basal area and forest height, respectively. The approach is quite close to the most "natural" way of calculating forest volume (e.g., Loetsch et al. 1973),

$$V = G \cdot H \cdot F, \tag{5}$$

where V = volume, G = basal area, H = mean height, and F = form factor. Thus, it satisfies the proposal by Treuhaft and Siqueira (2004) to express biomass from radar data with the plausible relationship, that

$$\text{biomass} \propto \text{vegetation height} \times \text{vegetation density}. \tag{6}$$

Given that the radar intensity return relates more to basal area than to biomass, height is the other crucial parameter for the monitoring of biomass to be incorporated. The adopted approach combining P-band backscatter with interferometric height thus comes close to a natural way of retrieving forest biomass.

In the biomass model, backscatter is not significant to the same level as interferometric height, because it contributes mainly to estimation of biomass stocks for secondary forests, whereas saturation occurs for primary forests. However, forest height would be expected to be firmly related to forest biomass for all successional stages, unless for initial regrowth. This is due to successional effects of quickly changing species composition in very young tropical forests. It takes years until the situation becomes more stable (Finegan 1996). In a study by Hyyppä et al. (2000), radar-based height measurements were verified to be the best single predictor of forest biomass, but the models performed even better when also including radar backscatter. Here, interferometric height outperforms radar backscatter by far in the estimation of biomass. Nevertheless, biomass is modeled as a linear combination of both backscatter and interferometric height to assure highest reliability.

Experiences with forest height measurements and links to biomass from high-quality interferometric SAR are rare for tropical environments (e.g., Hoekman and Varekamp 2001), although there have been many campaigns in temperate and boreal forests (e.g., Papathanassiou and Cloude 2001, Treuhaft and Siqueira 2004). Even in this research, where the collected data are not optimal, significant efforts had to be dedicated to the calibration of the interferometric models (Dutra et al. 2005), and the forest inventory data set includes only a few stands of medium height. (The study area was initially settled a short time ago, and there are no secondary forests older than ~25 years.) There is a distinct need to conduct additional research with high-quality airborne interferometric SAR data sets for the Amazon.

Literature Cited

CHAMBERS, J.Q., J. SANTOS, R.J. RIBEIRO, AND N. HIGUCHI. 2001. Tree damage, allometric relationships, and above-ground net primary production in central Amazon forest. Forest Ecol. Manage. 152:73–84.

DOBSON, M.C., F.T. ULABY, L.E. PIERCE, T.L. SHARIK, K.M. BERGEN, J. KELLNDORFER, J.R. KENDRA, E. LI, Y.C. LIN, A. NASHASHIBI, K. SARABANDI, AND P. SIQUEIRA. 1995. Estimation of forest biophysical characteristics in northern Michigan with SIR-C/X-SAR. IEEE Trans. Geosci. Remote Sens. 33(4):877–895.

DUTRA, L.V., M.T. ELMIRO, J.C. MURA, C.C. FREITAS, J.R. SANTOS, B.T.S. FILHO, P.C.G. DE ALBUQUERQUE, P.R. VIEIRA, AND F.F. GAMA. 2002. Assessment of digital elevation models obtained in Brazilian Amazon based on P and X-band airborne interferometric data. P. 3614–3616 *in* Proc. of the International Geoscience and Remote Sensing Symposium (IGARSS), Piscataway, N.J. (ed.). IEEE, Toronto, Canada.

FINEGAN, B. 1996. Pattern and process in neotropical secondary rain forests: The first 100 years of succession. TREE 11(3):119–124.

HOEKMAN, D.H., AND C. VAREKAMP. 2001. Observation of tropical rain forest trees by airborne high-resolution interferometric radar. IEEE Trans. Geosci. Remote Sens. 39(3):584–594.

HOFMANN, C., M. SCHWÄBISCH, S. OCH, C. WIMMER, AND J. MOREIRA. 1999. Multipath P-band interferometry—First results. *In* Proc. of 21st Canadian Symposium on Remote Sensing, June 21–24 1999. Ottawa, Canada.

HYYPPÄ, J., H. HYYPPÄ, M. INKINEN, M. ENGDAHL, S. LINKO, AND Y. ZHU. 2000. Accuracy comparison of various remote sensing data sources in the retrieval of forest stand attributes. Forest Ecol. Manage. 128:109–120.

IMHOFF, M.L. 1995. Radar backscatter and biomass saturation:

Ramifications for a global biomass inventory. IEEE Trans. Geosci. Remote Sens. 33(2):511–518.

KOSKINEN, J.T., T. PULLIAINEN, J.M. HYYPPÄ, M.E. ENGDAHL, AND M.T. HALLIKAINEN. 2001. The seasonal behavior of interferometric coherence in boreal forest. IEEE Trans. Geosci. Remote Sens. 39(4):820–829.

LE TOAN, T., A. BEAUDOIN, J. RIOM, AND D. GUYON. 1992. Relating forest biomass to SAR data. IEEE Trans. Geosci. Remote Sens. 30(2):403–411.

LOETSCH, F., F. ZÖHRER, AND K.E. HALLER. 1973. Forest inventory, Vol. 2. BLV Verlagsgesellschaft, München, Germany. 469 p.

LUCKMAN, A., J. BAKER, M. HONZÁK, AND R. LUCAS. 1998. Tropical forest biomass density estimation using JERS-1 SAR: Seasonal variation, confidence limits, and application to image mosaics. Remote Sens. Environ. 63:126–139.

NEEFF, T., AND J.R. DOS SANTOS. 2005. A growth model for secondary forest in Central Amazonia. For. Ecol. Manage. 216:270–282.

NELSON, B.W., R. MESQUITA, J.L.G. PEREIRA, S.G.A. SOUZA, G.T. BATISTA, AND L.B. COUTO. 1999. Allometric regressions for improved estimate of secondary forest biomass in the central Amazon. Forest Ecol. Manage. 117:149–167.

PAPATHANASSIOU, K.P., AND S.R. CLOUDE. 2001. Single-baseline polarimetric SAR interferometry. IEEE Trans. Geosci. Remote Sens. 39(11):2352–2363.

SANTOS, J.R., M.S.P. LACRUZ, L.S. ARAUJO, AND M. KEIL. 2002. Savanna and tropical rainforest biomass estimation and spatialization using JERS-1 data. Int. J. Remote Sens. 7:1217–1229.

TREUHAFT, R.N., AND P.R. SIQUEIRA. 2000. Vertical structure of vegetated land surfaces from interferometric and polarimetric radar. Radio Sci. 35(1):141–177.

TREUHAFT, R.N., AND P.R. SIQUEIRA. 2004. The calculated performance of forest structure and biomass estimates from interferometric radar. Wave. Random Media 14:345–358.